

Article

Study of a Thin Film Aluminum-Air Battery

Petros Katsoufis ¹, Maria Katsaiti ¹, Christos Mourelas ², Tatiana Santos Andrade ² ,
Vassilios Dracopoulos ³, Constantin Politis ⁴, George Avgouropoulos ^{1,*}  and
Panagiotis Lianos ^{2,*} 

¹ Department of Materials Science, University of Patras, 26500 Patras, Greece; Petroskatsouf@hotmail.com (P.K.); mairhcat11@gmail.com (M.K.)

² Department of Chemical Engineering, University of Patras, 26500 Patras, Greece; cmng3313@upnet.gr (C.M.); tsandrade@live.com (T.S.A.)

³ FORTH/ICE-HT, P.O. Box 1414, 26504 Patras, Greece; indy@iceht.forth.gr

⁴ Laboratory of High-tech Materials, University of Patras, 26500 Patras, Greece; politisxyz@gmail.com

* Correspondence: geoavg@upatras.gr (G.A.); lianos@upatras.gr (P.L.)

Received: 29 February 2020; Accepted: 19 March 2020; Published: 20 March 2020

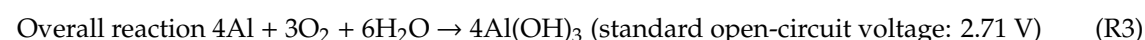
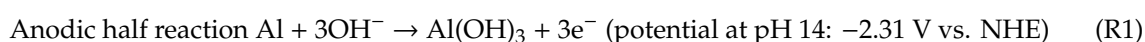


Abstract: A thin film aluminum-air battery has been constructed using a commercial grade Al-6061 plate as anode electrode, an air-breathing carbon cloth carrying an electrocatalyst as cathode electrode, and a thin porous paper soaked with aqueous KOH as electrolyte. This type of battery demonstrates a promising behavior under ambient conditions of 20 °C temperature and around 40% humidity. It presents good electric characteristics when plain nanoparticulate carbon (carbon black) is used as electrocatalyst but it is highly improved when MnO₂ particles are mixed with carbon black. Thus, the open-circuit voltage was 1.35 V, the short-circuit current density 50 mA cm⁻², and the maximum power density 20 mW cm⁻² in the absence of MnO₂ and increased to 1.45 V, 60 mA cm⁻², and 28 mW cm⁻², respectively, in the presence of MnO₂. The corresponding maximum energy yield during battery discharge was 4.9 mWh cm⁻² in the absence of MnO₂ and increased to 5.5 mWh cm⁻² in the presence of MnO₂. In the second case, battery discharge lasted longer under the same discharge conditions. The superiority of the MnO₂-containing electrocatalyst is justified by electrode electrochemical characterization data demonstrating reduction reactions at higher potential and charge transfer with much smaller resistance.

Keywords: Al-air battery; paper based thin film battery; MnO₂

1. Introduction

Aluminum-air (Al-air) batteries constitute a highly promising technology for powering electric vehicles and portable electronics. The principle of their operation can be described by the following reactions applicable to alkaline electrolytes [1,2]:



Al-air batteries are devices, which are very simple to construct and operate. In their most common version, they are made of an aluminum anode and a carbon cathode electrode in contact with an alkaline electrolyte. The dissolution of aluminum releases electrons which can flow in an external circuit and arrive at the cathode where they are consumed in oxygen reduction reactions. Oxygen may be provided by air, hence the Al-air functionality. An Al-air battery is in reality an Al-air fuel cell,

where the “fuel” is aluminum itself, which is consumed during device operation. Al-air batteries are very popular and this is justified by some important advantages: they offer relatively high open-circuit voltage (V_{OC} , cf. Reaction (3)); they are based on aluminum which is the third most abundant element in the Earth crust and can be additionally recovered by electrolysis of $Al(OH)_3$; and the theoretical specific energy density of Al-air batteries is around 8.1 kWh kg^{-1} , which is more than 10 times higher than that of commercial Li batteries [3,4]. Al-air batteries have been studied for several decades [1–6] and they may be considered a mature technology. However, they still attract a large research interest which extends over the materials used to make electrodes, the choice of electrolyte and electrolyte support, the electrocatalysts employed for oxygen reduction, the construction design, their stability etc. One design, which may be of particular interest in portable and wearable electronics, is Al-air thin film battery, for example, based on filter paper soaked with electrolyte [5,7–9]. This battery is very easy to build. It suffices to sandwich a porous paper soaked with an alkaline electrolyte between an aluminum sheet anode and a carbon cloth or carbon paper cathode to make a functional battery. These devices offer the additional advantage of flexible geometry [4,10]. In the present work, we have built such a battery using a simple design and have studied the conditions for improving its functionality.

The battery geometry is schematically represented by Figure 1. The two electrodes were pressed together by using appropriate plastic fittings and were separated by laboratory filter paper soaked with a solution of KOH. The anode was an aluminum plate and the cathode a carbon cloth carrying carbon black as basic electrocatalyst. This system was functional and did not necessitate any noble electrocatalyst to achieve its functionality. The characteristics of such a battery was then studied in terms of efficiency, power production capacity, and stability. Carbon cloth is an air breathing electrode and it obviously operates by oxygen reduction. Oxygen can be reduced either by Reaction (2), which is a four-electron process, or by the following reaction, which is a two-electron process:



Reaction (4) is easier to realize than Reaction (2) because it is a two-electron process and necessitates a less efficient electrocatalyst, even though it corresponds to a smaller V_{OC} . Subsequent reduction of H_2O_2 , for example, by the following reaction [11,12]



leads to the same effect as Reaction (2) but obviously by a slower process. A simple carbon cloth electrode covered with carbon black (i.e., nanoparticulate carbon) may then suffice to make a functional electrode and a functional device. This has been shown in previous works [1,2] and as it will be discussed below, it has been presently verified by the construction of thin film batteries. Nevertheless, the additional presence of a more efficient electrocatalyst does have beneficial effects on power production capacity. With this in mind, in the present work we studied the addition of MnO_2 as non-noble-metal electrocatalyst to operate the thin film Al-air battery. MnO_2 has been previously successfully employed as oxygen reduction electrocatalyst in several types of fuel cell devices including Al-air battery [13], Na-air battery [14], microbial fuel cells [15–18], and other types of fuel cells [19]. The present work will then also deal with the study of MnO_2 -loaded cathode electrodes which will be applied to thin film Al-air batteries. Finally, it must be underlined at this point that the present work studies a battery based on commercial low-cost aluminum, therefore, the proposed device may set the basis for a future commercial product.

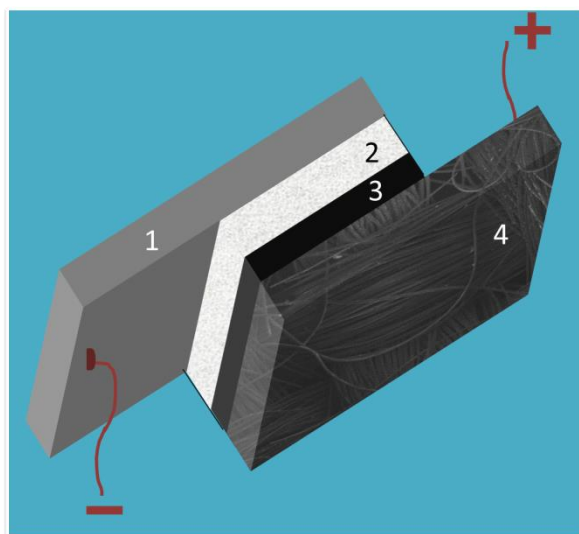


Figure 1. Schematic representation of the thin film Al-air battery: (1) aluminum plate; (2) filter paper soaked with electrolyte; (3) catalyst layer; and (4) carbon cloth electrode.

2. Materials and Methods

2.1. Materials

All materials were of reagent grade and were provided by Sigma-Aldrich unless otherwise specified. Thus Al-6061 was a donation from Alcoa Corp. (Pittsburgh, PA, USA), carbon cloth (CC) was purchased from Fuel Cell Earth (Wobum, MA, USA), and carbon black (CB) from Cabot Corporation (Vulcan XC72, Billerica, MA, USA).

2.2. Preparation of the Anode Electrode

The anode electrode was an aluminum Al-6061 plate of 1×1 cm active dimensions. It was mechanically polished before use in order to prepare a mirror-like surface, by employing a 4000 grit (European P-grade) SiC waterproof metallography polishing paper and then with $3 \mu\text{m}$ followed by 250 nm diamond paste.

2.3. Construction of the CB/CC and the MnO_2 -CB/CC Cathode Electrode

Carbon cloth was cut into pieces with similar active dimensions as Al plates, i.e., 1×1 cm. It was then covered (only one side) with carbon black. For this purpose, we prepared the following paste based on carbon black Vulcan XC72: 1 g of carbon black was mixed with 30 mL of distilled water by vigorous mixing in a laboratory mixer (more than 4000 r.p.m.) until it became a viscous paste. This paste was further mixed with 0.4 mL polytetrafluorethylene (Teflon 60% wt. dispersion in water) and then it was applied on the carbon cloth. This was achieved by first spreading the paste with a spatula, preheating for a few minutes at $80 \text{ }^\circ\text{C}$, and finally annealing for a few minutes in an oven at $340 \text{ }^\circ\text{C}$. The procedure was repeated once more to make sure that the carbon cloth was well covered with the hydrophobic carbon layer. In order to introduce MnO_2 , the same as above procedure was followed with the difference that further to the 1 g of CB, 0.5 g of a commercial MnO_2 powder (>99% purity) was also added after copiously grinding with a mortar (i.e., two parts of CB for one part of MnO_2). The choice of this ratio was made by optimization of the efficiency of the electrode and the stability of the material on the carbon cloth.

2.4. Description of the Device

The device is schematically shown in Figure 1. A filter paper 0.16 mm thick (MN-615, Macherey-Nagel, Duren, Germany) was cut in the appropriate dimensions, was soaked with 2 M

aqueous KOH, and was sandwiched between the aluminum plate and the carbon cloth electrode. Appropriate plastic supports were machined to hold the three items tight together. The active dimension was 1×1 cm. The side of the carbon cloth that was covered with the catalyst was in contact with the filter paper while the other side was exposed to the ambient air. All measurements were made under ambient conditions of $20\text{ }^{\circ}\text{C}$ and 40% humidity without sealing the device.

2.5. Measurements and Characterizations

Polishing of the aluminum surface was monitored by a high-resolution optical microscope Reichert MeF 2 carrying an objective Plan Oel 125/1.35 by using Canada balsam immersion oil with a refractive index of $n = 1$. Current-voltage curves and potentiometric or amperometric measurements were made with an Autolab potentiostat PGSTAT128N and FESEM images with a Zeiss SUPRA 35 VP 143 microscope.

3. Results and Discussion

3.1. Material Characterization

The aluminum Al-6061 anode electrode was a plate cut from a bigger sample and was machined to obtain appropriate size so that its active dimensions were 1 cm^2 , as already said. Before use, the plate was polished, as detailed in Section 2. The same material was employed and characterized in a previous publication [2].

The counter electrode was made of a carbon cloth on which carbon black was deposited as detailed in Section 2.3 (CB/CC). Figure 2A shows its image revealing the carbon black nanostructure. When carbon black was mixed with ground MnO_2 particles (MnO_2 -CB/CC), the obtained blend gave the image of Figure 2B where the two phases are easily distinguished. MnO_2 came into the blend as elongated particles with the longer dimension larger than $1\text{ }\mu\text{m}$. These particles were obviously produced by grinding and then vigorously mixing larger particles, which seem to be composed of MnO_2 flakes, as revealed by the image of Figure 2C.

Finally, the structure of the filter paper is also demonstrated in Figure 2D showing the inter-weaving of cellulose filaments.

3.2. Electric Characteristics of the Thin Film Al-Air Battery

The electric characteristics of the above described battery can be seen in Figure 3. The battery reached a V_{OC} of around 1.4 V while the short circuit current density J_{SC} was 50 mA cm^{-2} in the absence and a little more than 60 mA cm^{-2} in the presence of MnO_2 . The presence of the metal oxide had then a substantial effect on device performance. This difference was more pronounced in the case of power density, the maximum of which increased by 40% in the presence of the metal oxide particles. Indeed, it was approximately 20 mW cm^{-2} in the absence and increased to 28 mW cm^{-2} in the presence of MnO_2 . A plain CB/CC electrode then makes a battery with satisfactory performance, but it enjoys an even better performance when manganese oxide is mixed with carbon black. This result justifies the employment of MnO_2 as oxygen reduction electrocatalyst both in the present case as well as in other fuel cell applications, as already discussed [13–19]. The appearance of the polarization curve, more specifically, the fact that current density continuously increased with voltage decrease and did not demonstrate an extremum is a rough index of the state of the electrolyte in the device. Thus, it shows that the electrolyte remains in a quasi-liquid state within the pores of the filter paper and it does not create hard constraints to ionic conductivity. In the opposite case, that is for a quasi-solid electrolyte, the ionic conductivity is limited, and the polarization curve demonstrates an extremum [5–7] while the observed current density is smaller. Obviously, the present case practically deals with a thin film liquid electrolyte. The question then is how steady and for how long such a battery will function without sealing under ambient conditions. This has been studied by performing battery discharge tests by choosing several steady current density conditions as detailed in the next paragraph.

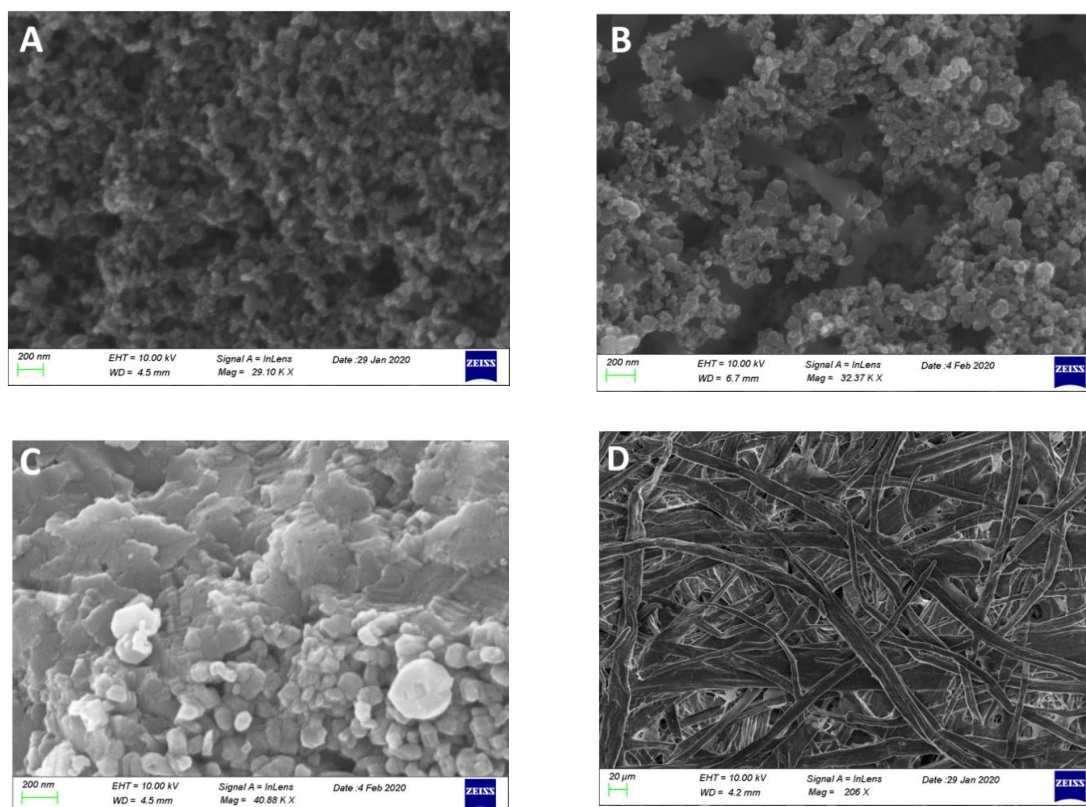


Figure 2. FE-SEM images of carbon black nanoparticles (A); carbon black mixed with ground MnO₂ particles (B); MnO₂ particles (C); and the structure of the paper before soaking with electrolyte (D). The scale bar is 200 nm in (A–C) and 20 μm in (D).

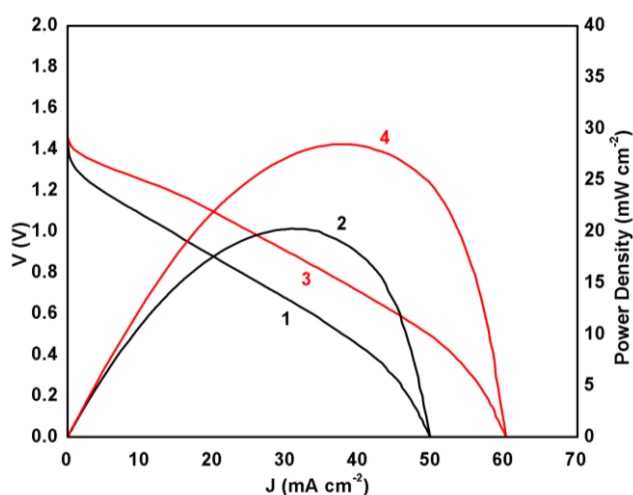


Figure 3. Polarization curves (1, 3) and power density curves (2, 4) for the presently studied Al-air battery. Curves (1) and (2) correspond to a carbon black/carbon cloth (CB/CC) cathode and curves (3) and (4) to a MnO₂-CB/CC cathode electrode.

Figure 4 shows battery discharge in the absence of MnO₂. The open-circuit voltage (at current zero) was stable for several hours. However, the battery was discharged in about 1.5 h when running at 1 mA cm⁻². As expected, discharging was faster at higher current densities. The total energy yield can be calculated by measuring the area under each curve and it was 1.8, 4.9, and 2.1 mWh cm⁻², when discharging was monitored at 1, 5, and 20 mA cm⁻², respectively.

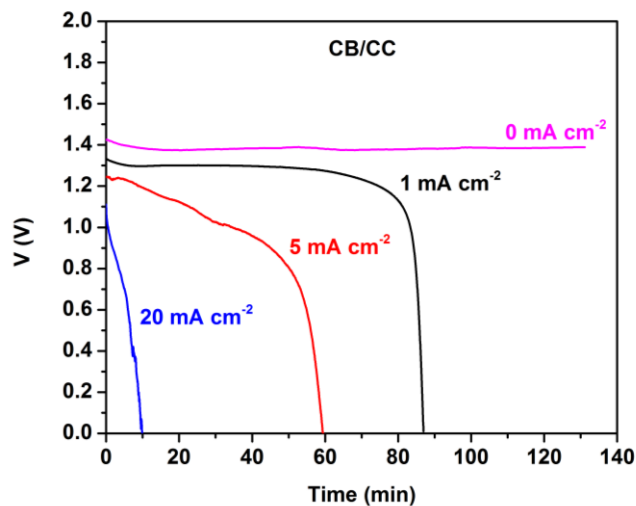


Figure 4. Potentiometry curves at various current densities for the Al-air thin film battery employing a plain CB/CC cathode without MnO_2 .

Figure 5 shows corresponding battery discharge data in the presence of MnO_2 . Again, V_{OC} was stable for several hours. It now took a longer time to discharge the battery for the same current density values than in the absence of MnO_2 . The corresponding total energy yield was 2.5, 5.5, and 2.7 mWh cm^{-2} , when discharging was monitored at 1, 5, and 20 mA cm^{-2} , respectively. Once more the beneficial presence of manganese oxide is clearly demonstrated by these data. The total energy yield should be approximately the same no matter how much the current density is. It is interesting to find out that in both battery cases, i.e., both in the presence and in the absence of MnO_2 , discharging at 5 mA cm^{-2} yielded much higher energy than discharging at 1 or 20 mA cm^{-2} . The most plausible explanation for this behavior is based on the data of [20]. In Al-air batteries generation of electrons by oxidation of Al is always in competition with corrosion, which is described by the following reaction:

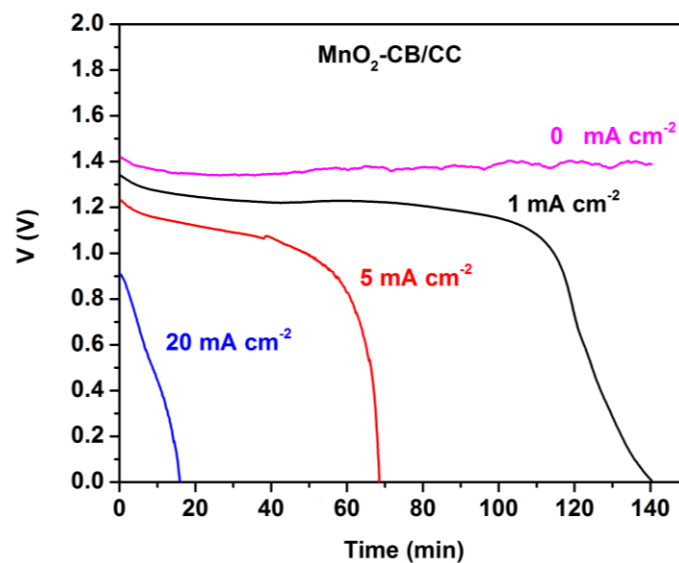


Figure 5. Potentiometry curves at various current densities for the Al-air thin film battery employing a MnO_2 -CB/CC cathode.

Competition means that when the current produced by Reaction (1) is high, corrosion becomes less important. The opposite is true when the current is low. However, when the current is high, the voltage is low, as seen in Figures 4 and 5. These opposing trends create a maximum in the total energy yield of the battery as a function of current, hence the maximum observed in the present case, i.e., when the discharge current density was 5 mA cm^{-2} .

The electrochemical factors that make the presence of MnO_2 enhance battery performance are discussed in the next subsection.

3.3. Electrochemical Characterization of the MnO_2 -CB/CC vs. CB/CC Electrode

The above results show that the CB/CC and the MnO_2 -CB/CC electrodes have different capacities in carrying out reduction reactions, in particular, oxygen reduction. A direct comparison between them can be qualitatively obtained by the polarization curves of Figure 6. Comparison is additionally made with a plain carbon cloth electrode under the same conditions. The three electrodes were tested as working electrodes, with a Pt foil as counter and an Ag/AgCl as reference electrode, using an alkaline electrolyte. The data were plotted vs. reversible hydrogen electrode (RHE) by taking into account the pH value of the electrolyte and the potential of the Ag/AgCl electrode (0.2 V). The importance of the presence of carbon black (CB) and, furthermore, that of the MnO_2 particles is obvious from these data since the onset of cathodic currents appears at more positive potentials in going from plain carbon cloth to CB/CC and then to MnO_2 -CB/CC. Even though, these data are approximate and cannot safely determine the potential of the reduction reaction in each case, they do show that the presence of MnO_2 particles better approaches oxygen reduction by Reaction (2) than plain CB/CC or even better than plain CC.

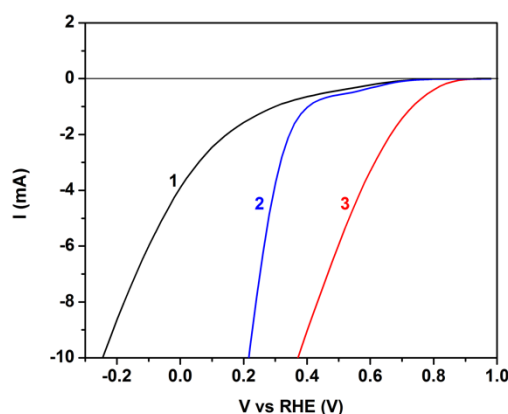


Figure 6. Polarization curves obtained by using one of the following three different electrodes as working electrode, a Pt foil as counter electrode and an Ag/AgCl as reference electrode: (1) plain carbon cloth; (2) CB/CC; and (3) MnO_2 -CB/CC. The electrolyte was 0.5 M KOH.

The superiority of the MnO_2 -CB electrocatalyst was also demonstrated by electrochemical impedance measurements, the results of which are shown in Figure 7. Symmetric devices were employed using only CC/CB or MnO_2 -CB/CC electrodes in contact with aqueous KOH electrolyte, at zero bias and by changing frequency between 100 kHz and 0.1 Hz. A simple circuit R-RC fitted well the experimental data in a Nyquist plot providing an electron transfer resistance which was 13.7 kohm in the case of CB/CC and decreased to 1.3 kohm in the presence of MnO_2 . This trend was also observed with intermediate MnO_2 loads, i.e., the charge transfer resistance decreased with the quantity of added MnO_2 . It is then more than obvious that transfer of electrons in solution is greatly facilitated in the presence of the metal oxide, therefore, MnO_2 -CB/CC makes a better cathode electrode for the present application.

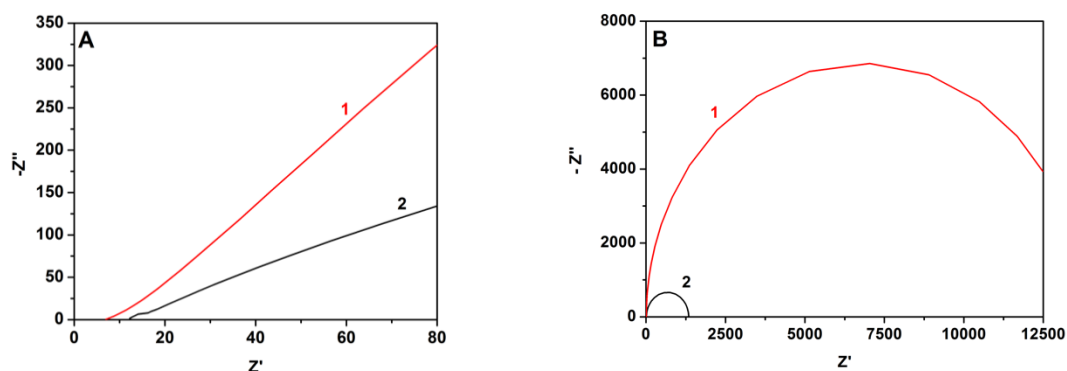


Figure 7. Experimental data for impedance measurements (A) and corresponding Nyquist plots (B) for symmetric cells using (1) CB/CC and (2) MnO₂-CB/CC electrodes. The electrolyte was 0.5 M KOH.

4. Conclusions

A thin film Al-air battery based on porous paper soaked with aqueous KOH electrolyte and sandwiched between a technical grade commercial Al-6061 anode and a carbon cloth cathode carrying various electrocatalysts makes a functional device with satisfactory power yield records. The performance of the battery substantially increased when a mixture of MnO₂ with nanoparticulate carbon was employed as oxygen reduction electrocatalyst. These results are in accordance with electrochemical characterization data of CB/CC and MnO₂-CB/CC electrodes which demonstrated the beneficial effects of the presence of MnO₂ particles.

Author Contributions: Investigation, P.K., M.K., C.M., T.S.A. and V.D.; supervision, C.P. and G.A.; conceptualization P.L. All authors have read and agreed to the published version of the manuscript.

Funding: This research received no external funding.

Acknowledgments: T.S.A. Acknowledges support through a scholarship provided by the Coordenação de Aperfeiçoamento de Pessoal de Nível Superior-Brasil (Capes)-Finance Code 001 that allowed her stay in the University of Patras.

Conflicts of Interest: The authors declare no conflict of interest.

References

1. Raptis, D.; Seferlis, A.K.; Mylona, V.; Politis, C.; Lianos, P. Electrochemical hydrogen and electricity production by using anodes made of commercial aluminum. *Int. J. Hydrog. Energy* **2019**, *44*, 1359–1365. [[CrossRef](#)]
2. Katsoufis, P.; Mylona, V.; Politis, C.; Avgouropoulos, G.; Lianos, P. Study of some basic operation conditions of an Al-air battery using technical grade commercial aluminum. *J. Power Sources* **2020**, *450*, 227624. [[CrossRef](#)]
3. Liu, Y.; Sun, Q.; Li, W.; Adair, K.R.; Li, J.; Sun, X. A comprehensive review on recent progress in aluminium—Air batteries. *Green Energy Environ.* **2017**, *2*, 246–277. [[CrossRef](#)]
4. Zhu, C.; Ma, Y.; Zang, W.; Guan, C.; Liu, X.; Pennycook, S.J.; Wang, J.; Huang, W. Conformal dispersed cobalt nanoparticles in hollow carbon nanotube arrays for flexible Zn-air and Al-air batteries. *Chem. Eng. J.* **2019**, *369*, 988–995. [[CrossRef](#)]
5. Wang, Y.; Pan, W.; Kwok, H.; Lu, X.; Leung, D.Y.C. Low cost Al-air batteries with paper-based solid electrolyte. *Energy Procedia* **2019**, *158*, 522–527. [[CrossRef](#)]
6. Eftekhari, A.; Corrochanoc, P. Electrochemical energy storage by aluminum as a lightweight and cheap anode/charge carrier. *Sustain. Energy Fuels* **2017**, *1*, 1246–1265. [[CrossRef](#)]
7. Wang, Y.; Pan, W.; Kwok, H.Y.H.; Zhang, H.; Lu, X.; Leung, D.Y.C. Liquid-free Al-air batteries with paper-based gel electrolyte: A green energy technology for portable electronics. *J. Power Sources* **2019**, *437*, 226896–226907. [[CrossRef](#)]
8. Wang, Y.; Kwok, H.Y.H.; Pan, W.; Zhang, Y.; Zhang, H.; Lu, X.; Leung, D.Y.C. Combining Al-air battery with paper-making industry, a novel type of flexible primary battery technology. *Electrochim. Acta* **2019**, *319*, 947–957. [[CrossRef](#)]

9. Di Palma, T.M.; Migliardini, F.; Gaele, M.F.; Corbo, P. Physically cross-linked xanthan hydrogels as solid electrolytes for Al/air batteries. *Ionics* **2019**, *25*, 4209–4217. [[CrossRef](#)]
10. Wang, M.; Li, Y.; Fang, J.; Villa, C.J.; Xu, Y.; Hao, S.; Li, J.; Liu, Y.; Wolverton, C.; Chen, X.; et al. Superior Oxygen Reduction Reaction on Phosphorus—Doped Carbon Dot/Graphene Aerogel for All-Solid-State Flexible Al–Air Batteries. *Adv. Energy Mater.* **2019**, *10*, 1902736. [[CrossRef](#)]
11. Hasvold, O.; Johansen, K.H.; Mollestad, O.; Forseth, S.; Størkersen, N. The alkaline aluminium hydrogen peroxide power source in the Hugin II unmanned underwater vehicle. *J. Power Sources* **1999**, *80*, 254–260. [[CrossRef](#)]
12. Zhang, H.; Yang, Y.; Liu, T.; Chang, H. Boosting the Power-Generation Performance of Micro-Sized Al-H₂O₂ Fuel Cells by Using Silver Nanowires as the Cathode. *Energies* **2018**, *11*, 2316. [[CrossRef](#)]
13. Kuo, Y.L.; Wu, C.C.; Chang, W.S.; Yang, C.R.; Chou, H.L. Study of Poly (3, 4-ethylenedioxythiophene)/MnO₂ as Composite Cathode Materials for Aluminum-Air Battery. *Electrochim. Acta* **2015**, *176*, 1324–1331. [[CrossRef](#)]
14. Khan, Z.; Park, S.; Hwang, S.M.; Yang, J.; Lee, Y.; Song, H.-K.; Kim, Y.; Ko, H. Hierarchical urchin-shaped α -MnO₂ on graphene-coated carbon microfibers: A binder-free electrode for rechargeable aqueous Na–air battery. *NPG Asia Mater.* **2016**, *8*, 294. [[CrossRef](#)]
15. Zhang, S.; Su, W.; Wei, Y.; Liu, J.; Li, K. Mesoporous MnO₂ structured by ultrathin nanosheet as electrocatalyst for oxygen reduction reaction in air-cathode microbial fuel cell. *J. Power Sources* **2018**, *401*, 158–164. [[CrossRef](#)]
16. Tremouli, A.; Karydogiannis, I.; Pandis, P.K.; Papadopoulou, K.; Argirusis, C.; Stathopoulos, V.N.; Lyberatos, G. Bioelectricity production from fermentable household waste extract using a single chamber microbial fuel cell. *Energy Procedia* **2019**, *161*, 2–9. [[CrossRef](#)]
17. Majidi, M.R.; Farahani, F.S.; Hosseini, M.; Ahadzadeh, I. Low-cost nanowired α -MnO₂/C as an ORR catalyst in air-cathode microbial fuel cell. *Bioelectrochemistry* **2019**, *125*, 38–45. [[CrossRef](#)] [[PubMed](#)]
18. Priya, A.D.; Setty, Y.P. Effect of MnO₂: rGO ratio on the performance of a microbial fuel cell: An experimental optimization study. *Energy Source Part A* **2019**, *41*, 600–610. [[CrossRef](#)]
19. Huang, B.; Zhang, X.; Cai, J.; Liu, W.; Lin, S. A novel MnO₂/rGO composite prepared by electrodeposition as a non-noble metal electrocatalyst for ORR. *J. Appl. Electrochem.* **2019**, *49*, 767–777. [[CrossRef](#)]
20. Hopkins, B.J.; Shao-Horn, Y.; Hart, D.P. Suppressing corrosion in primary aluminum—Air batteries via oil displacement. *Science* **2018**, *362*, 658–661. [[CrossRef](#)] [[PubMed](#)]



© 2020 by the authors. Licensee MDPI, Basel, Switzerland. This article is an open access article distributed under the terms and conditions of the Creative Commons Attribution (CC BY) license (<http://creativecommons.org/licenses/by/4.0/>).